THE JOURNAL OF BIOLOGICAL CHEMISTRY VOL. 284, NO. 40, pp. 27533–27543, October 2, 2009

Wnt-5a-induced Phosphorylation of DARPP-32 Inhibits Breast Cancer Cell Migration in a CREB-dependent Manner*

Received for publication, November 21, 2008, and in revised form, July 25, 2009 Published, JBC Papers in Press, August 3, 2009, DOI 10.1074/jbc.M109.048884

Christian Hansen[‡], Jillian Howlin[‡], Anders Tengholm[¶], Oleg Dyachok[¶], Wolfgang F. Vogel[‖†], Angus C. Nairn[**], Paul Greengard[‡‡], and Tommy Andersson[‡1]

*From [‡]Experimental Pathology, Department of Laboratory Medicine, Lund University, CRC, 205 02 Malmö, Sweden, the [¶]Department of Medical Cell Biology, Uppsala University, BMC, SE-751 23 Uppsala, Sweden, the [‖]Department of Laboratory Medicine and Pathobiology, University of Toronto, Toronto, Ontario M5S 1A8, Canada, the **Department of Psychiatry, Yale University School of Medicine, New Haven, Connecticut 06508, and the [‡‡]Laboratory for Molecular and Cellular Neuroscience, Rockefeller University, New York, New York 10021*

Tumor cell migration plays a central role in the process of cancer metastasis. We recently identified dopamine and cAMP-regulated phosphoprotein of 32 kDa (DARPP-32) as an antimigratory phosphoprotein in breast cancer cells. Here we link this effect of DARPP-32 to Wnt-5a signaling by demonstrating that recombinant Wnt-5a triggers cAMP elevation at the plasma membrane and Thr34-DARPP-32 phosphorylation in MCF-7 cells. In agreement, both protein kinase A (PKA) inhibitors and siRNA-mediated knockdown of Frizzled-3 receptor or $G\alpha_s$ expression abolished Wnt-5a-induced phosphorylation of DARPP-32. Furthermore, Wnt-5a induced DARPP-32-dependent inhibition of MCF-7 cell migration. Phospho-Thr-34-DARPP-32 interacted with protein phosphatase-1 (PP1) and potentiated the Wnt-5a-mediated phosphorylation of CREB, a well-known PP1 substrate, but had no effect on CREB phosphorylation by itself. Moreover, inhibition of the Wnt-5a/DARPP-32/CREB pathway, by expression of dominant negative CREB (DN-CREB), diminished the antimigratory effect of Wnt-5a-induced phospho-Thr-34-DARPP-32. Phalloidin-staining revealed that that the presence of phospho-Thr-34-DARPP-32 in MCF-7 cells results in reduced filopodia formation. In accordance, the activity of the Rho GTPase Cdc42, known to be crucial for filopodia formation, was reduced in MCF-7 cells expressing phospho-Thr-34-DARPP-32. The effects of DARPP-32 on cell migration and filopodia formation could be reversed in T47D breast cancer cells that were depleted of their endogenous DARPP-32 by siRNA targeting. Consequently, Wnt-5a activates a Frizzled-3/$G\alpha_s$/cAMP/PKA signaling pathway that triggers a DARPP-32- and CREB-dependent antimigratory response in breast cancer cells, representing a novel mechanism whereby Wnt-5a can inhibit breast cancer cell migration.

Breast cancer is the most common form of cancer in women. Whereas the prognosis for breast cancer patients without local or distal dissemination is relatively favorable, the prognosis is considerably worse once distal metastasis has been established. It is therefore imperative to identify molecular targets and develop novel antimetastatic therapies that will stop, reduce, or delay the dissemination and growth of breast cancer metastasis.

We recently isolated the dopamine and cAMP-regulated phosphoprotein of 32 kDa (DARPP-32),[2] from a human breast expression library, as a DDR1-binding partner (1). Introduction of DARPP-32 in breast cancer cells lacking endogenous expression of this protein inhibited cell migration in a phospho-Thr-34-DARPP-32-dependent manner (1). DARPP-32 was originally identified 25 years ago as a dopamine and cAMP target enriched in dopaminoceptive neurones (2). Since then, a large body of work has shown that DARPP-32 is crucial for signal transmission by a wide array of neurotransmitters and drugs of abuse. DARPP-32 can act as either a phosphatase inhibitor or a kinase inhibitor depending on its phosphorylation state. Phosphorylation of Thr-34 by protein kinase A (PKA) converts DARPP-32 into a potent inhibitor of protein phosphatase-1 (PP1) (3), whereas phosphorylation at Thr-75 by Cdk5 turns DARPP-32 into an inhibitor of PKA (4). Downstream of DARPP-32 it has been shown that the activity of CREB and c-fos are strongly attenuated in DARPP-32 knockout mice (5). Despite the substantial amount of work done on DARPP-32 over the past 25 years, the role of this phosphoprotein outside the neuronal system has only recently started to be explored.

Regarding the role of DARPP-32 in cancer, overexpression of DARPP-32 has been reported in gastric, colon, and prostate cancer (6, 7). In contrast, patients with esophageal squamous cell carcinoma that lacks DARPP-32 expression have reduced survival when compared with patients with DARPP-32-expressing esophageal squamous cell carcinomas (8, 9). Furthermore, DARPP-32 is needed to get a fully differentiated thyroid cell phenotype, and transformation of thyroid cells by constitu-

* This work was supported by grants from the Swedish Cancer Foundation (to T. A.), the Swedish Research Council (to T. A. and A. T.), the U-MAS Research Foundations (to T. A.), the Gunnar Nilsson's Cancer Foundation (to T. A.), the Royal Physiographic Society in Lund (to C. H.), Magnus Bergvall's Foundation (to A. T.), the Canada Research Chair Program (to W. V.), and in part, by National Institutes of Health Grant MH074866 (to A. N. and P. G.).

† The authors dedicate this article to the memory of Dr. Wolfgang F. Vogel, deceased on the 5th of December 2007.

[1] To whom correspondence should be addressed. Tel: 46-40-391167; Fax: 46-40-391177; E-mail: tommy.andersson@med.lu.se.

[2] The abbreviations used are: DARPP-32, cAMP-regulated phosphoprotein of 32 kDa; PP1, protein phosphatase-1; PKA, protein kinase A; DN-CREB, dominant negative CREB; CREB, cAMP response element-binding; rWnt-5a, recombinant rWnt-5a; rWnt-3a, recombinant Wnt-3a; PBS, phosphate-buffered saline; GST, glutathione *S*-transferase; GFP, green fluorescent protein; YFP, yellow fluorescent protein; CFP, cyan fluorescent protein.

tively activated Ras resulted in a loss of DARPP-32 expression (10). Thus, the role of DARPP-32 in cancer is somewhat uncertain, and little is known about the cell signaling mechanisms behind a possible suppressor or promotor role of DARPP-32 in cancer.

Wnt-5a is a non-canonical member of the Wnt family of secreted glycoproteins that acts through the family of Frizzled G-protein-coupled receptor, Ror2, and co-receptors such as, LRP5/6, to mediate important events during development and cancer (11–15). In the breast, the non-transforming Wnt-5a has been shown to inhibit epithelial cell migration (16), and in breast cancer, expression of Wnt-5a has been shown to be a predictor of longer disease-free survival (17). Wnt-5a expression has been shown to increase activation of the receptor tyrosine kinase DDR1 in breast epithelial cells upon plating on collagen (18). As DDR1 is a collagen-binding adhesion receptor important for cell migration (19), and its binding partner DARPP-32 is a phospho-dependent antimigratory molecule (1), we wanted to test whether the functional overlaps between DARPP-32 and Wnt-5a, could be a result of Wnt-5a acting upstream in the signaling process leading to DARPP-32 phosphorylation.

Here we demonstrate that Wnt-5a can trigger a Frizzled-3/Gαs/cAMP signal that results in PKA-dependent phosphorylation of DARPP-32. Furthermore, we show that phospho-DARPP-32 potentiates Wnt-5a-mediated CREB activity and suppresses filopodia formation.

EXPERIMENTAL PROCEDURES

Cell lines, Reagents, Plasmids, and Transfection—All cell lines were obtained from ATCC, except for HB2 cells that were kindly provided by Dr. J. Taylor-Papadimitriou (Imperial Cancer Research Fund, United Kingdom). Recombinant Wnt-5a was from R&D and H89, RPcAMP, and forskolin from Sigma. The Myc-DARPP-32 expression vector was generated by inserting rat DARPP-32 cDNA, amplified by primers with flanking EcoRI and BglII sites, into the corresponding sites of the pCMVMyc vector. The generation of the T34A mutation within DARPP-32 was described previously (3). DN-CREB expression plasmid was a kind gift from Dr. Richard Goodman; Vollum Institute, Portland OR. Cells were transiently transfected with plasmids using oligofectamine according to the manufacturer's protocol (Invitrogen). To determine transfection efficiency, we used an EGFP-coding plasmid and reproducibly found a transfection rate of at least 55%. siRNA transfection was done using Lipofectamine according to the manufacturer's protocol. siRNA targeting DARPP-32 and $G\alpha_S$ were both from Santa Cruz Biotechnology.

Measurements of Near Plasma Membrane cAMP Concentration—The cAMP concentration in the subplasma membrane space was measured with evanescent wave microscopy and a fluorescent biosensor as previously described (20). In brief, the full-length PKA catalytic Cα subunit was labeled with yellow fluorescent protein (Cα-YFP) and a truncated PKA-RIIβ regulatory subunit was labeled with cyan fluorescent protein and targeted to the plasma membrane via a covalent lipid modification (ΔRIIβ-CFP-CAAX). The two constructs were transfected into MCF-7 cells growing on cover slips to allow expression of the fusion proteins for 24–48 h. The cells were then transferred to a buffer containing 125 mM NaCl, 4.8 mM KCl, 1.3 mM $CaCl_2$, 1.2 mM $MgCl_2$, 5.5 mM glucose, and 25 mM HEPES with pH adjusted to 7.4 with NaOH, and incubated for 30 min at 37 °C. Plasma membrane association of the fluorescent protein-tagged PKA subunits were measured using an evanescent wave microscopy setup built around an E600FN upright microscope (Nikon, Kanagawa, Japan). cAMP concentration was expressed as the ratio of CFP over YFP fluorescence after background subtraction. To compensate for the variability in expression levels of the two fusion proteins, the basal ratio was normalized to unity. The outlined cAMP traces are representative of 8–12 separate experiments.

Migration Assay—Boyden-chamber assay: Transwell wells (Costar) were coated with human collagen I (20 μg/ml) for 1 h at 37 °C. Cells were detached with trypsin and washed with serum-containing medium. 5000 cells were added to the upper chamber in a total volume of 200 μl of serum-free medium supplemented with 5 μg/ml bovine serum albumin. The same medium was present in the lower chamber. After 18 h, cells migrated through the porous membrane were stained with crystal violet and counted. Each experiment was done in triplicate, repeated 6–8 times, and statistical significances were evaluated by paired Student's *t* test (depicted as *, $p < 0.05$ or **, $p < 0.01$).

Wound Healing Assay—6-well plates were coated with human collagen I (20 μg/ml) for 1 h at 37 °C, and cells were plated and allowed to grow into a confluent layer. A wound was inflicted by making a scratch through the confluent layer of cells with a pipette tip. Cells were incubated in serum-free medium during the time span of the wound healing. A picture for each scratch was taken at the same area of cells at 0 and 24 h, and wound healing was measured as a percentage of wound area closed. Each experiment was done in duplicate, repeated 9–12 times, and statistical significances were evaluated by paired Student's *t* test (depicted as *, $p < 0.05$ or **, $p < 0.01$).

Western Blotting and Immunoprecipitation—For Western blotting, cells were either lysed directly in 1× Laemmli buffer and boiled for 5 min or lysed with buffer containing 1% Nonidet P-40, 20 mM Tris (pH 7.4), 150 mM NaCl, 5 mM EDTA, 5 mM EGTA, 2 mM sodium orthovanadate, 4 μg/ml leupeptin, 2 mM Pefabloc (Roche), 20 μg/ml aprotinin, and 5 mM NaF for 15 min on ice, centrifuged at 14,000 × *g* for 10 min, and then the pellet was resuspended in Laemmli buffer and boiled for 5 min. For immunoprecipitation, following lysis and centrifugation as above, the lysates were precleared with protein A-Sepharose at 4 °C for 30 min. Supernatants were incubated with 1–3 μg of antibody for 1 h, another aliquot of protein A-Sepharose added and incubated for 1 h. Immunocomplexes were washed three times with buffer, resuspended in Laemmli buffer and boiled for 5 min. Proteins were separated on 6, 8, or 10% polyacrylamide gels and subjected to Western blot transfer. Primary antibodies used for Western blotting were anti-DARPP-32 (H62, Santa Cruz Biotechnology), anti-phospho-Ser-133-CREB (Calbiochem), anti-CREB (48H2, Cell Signaling), anti-PP1 (E9, Santa Cruz Biotechnology, anti-actin (Sigma), anti-α-tubulin (Santa Cruz Biotechnology), anti-$G\alpha_S$ (Santa Cruz Biotechnology), and anti-Myc (Calbiochem). Phosphospecific

antibodies for Thr-34 and Thr-75 in DARPP-32 were described previously (21, 22). The anti-Frizzled-3 antibody, provided by Dr. Jeffrey Rubin, has been described previously (23). Secondary goat anti-rabbit and goat anti-mouse, horseradish peroxidase-conjugated antibodies were from Dako. All blots shown in this study are representative of at least three separate experiments.

Immunofluorescent Staining—Glass slides were coated with human collagen I (20 μg/ml) for 1 h at 37 °C, and cells transfected with wtDARPP-32 or T34A-DARPP-32 expression vector were detached and allowed to adhere onto the collagen-coated slides overnight at 37 °C. Cells were left non-stimulated or stimulated with forskolin and fixed in 4% paraformaldehyde for 15 min, washed three times in PBS, before permeabilization with 0.5% Triton X-100 for 5 min. Subsequently, the slides were washed three times with PBS and blocked 1 h in 3% bovine serum albumin (BSA) in PBS. The slides were incubated with primary antibody in 3% BSA in PBS for 1 h at room temperature. Following three washes with PBS, the slides were incubated with fluorescently labeled secondary antibody and washed three times in PBS. The cover slips were mounted on glass slides with a fluorescence-mounting medium. Fluorescently labeled Alexa goat anti-mouse 488, Alexa goat anti-rabbit 568, and Alexa fluor 488 phalloidin were all purchased from Invitrogen.

Quantitative Analysis of Filopodia—To compensate for differences in cell size, we counted the filopodia and expressed their numbers per 20-μm plasma membrane. Areas where cells were adhered to neighboring cells were not counted as these regions were typically devoid of filopodia. The cells were divided into 3 categories: Few, less than 3 filopodia per 20 μM; medium, 3–6 filopodia per 20 μM; and many, more than 6 filopodia per 20 μM. The cells were randomly selected and at least 50 of each cell type (stained and non-stained for DARPP-32) were counted in each experiment. Experiments were repeated five times, and statistical significances were evaluated by paired Student's *t* test (depicted as *, $p < 0.05$; **, $p < 0.01$; or ***, $p < 0.001$).

GST Pull-down Assay —The cDNA of the Cdc42-binding domain from PAK1B (PAKcrib; amino acids 56–267) was cloned into bacterial expression vector pGEX-2T and expressed in *Escherichia coli* as a fusion protein with glutathione *S*-transferase (GST). MCF-7 cells transfected with either DARPP-32 expression vector or empty vector control were replated onto collagen-coated plates and lysed after 0–60 min in a buffer composed of 50 mM Tris-HCl, pH 7.5, 1% Triton X-100, 100 mM NaCl, 10 mM $MgCl_2$, 5% glycerol, 1 mM Na_3VO_4, and protease inhibitors (20 μg/ml aprotinin; 1 mg/ml each of pepstatin, leupeptin, and antipain; 2.5 mM benzamidine; 2 mM Pefabloc). The GST-PAK1B fusion protein was coupled to glutathione-Sepharose beads for 1 h, and then the beads were washed and subsequently added to the clarified MCF-7 lysates. After 1 h, the beads were collected by centrifugation and washed three times in 25 mM Tris-HCl, pH 7.5, 1% Triton X-100, 1 mM dithiothreitol, 100 mM NaCl, and 30 mM $MgCl_2$. Next, the beads were resuspended in Laemmli sample buffer, boiled for 5 min, and subjected to 14% SDS-PAGE.

RNA Extraction and RT-PCR—RNA extraction was performed in a designated clean RNA area with the addition of 500 μl of TRIzol to each sample. 100 μl of chloroform was then added, and samples centrifuged at 4 °C at 8,000 × *g* for 10 min. 250 μl of isopropyl alcohol was added to the clear upper phase, and samples centrifuged for 15 min at 4 °C at 8,000 × *g*. The supernatant was removed, and the pellet was washed in 75% ethanol and resuspended in DEPC-treated water. RNA was treated with DNase 1 (Invitrogen) at 37 °C for 15 min. The RNA concentration was measured using a Nanodrop Spectrophotometer ND-1000 (Bio-Rad). cDNA was synthesized from 1 μg of total RNA using M-MuLV reverse transcriptase (Fermentas) in a MJ Mini Personal Thermal Cycler (Bio-Rad). The primers used were: Frizzled-2, 5′-ACATCGCCTACAACCAGACC-3′ and 5′-ACGCTCGCCCAGAAACTTGTAGC-3′; Frizzled-3, 5′-GGCTGTGTCAGCGGGCT-3′ and 5′-TCTTCAGGCCA-AGGAACACC-3′; Frizzled-4, 5′-CCTGGAAGCATTCAAC-TCAGC-3′, and TGTGGTTGTGGTCGTTCTGTG-3′; Frizzled-5, 5′-ACACCCGCTCTACAACAAGG-3′ and 5′-CGT-AGTGGAGGATGTGGTTGTGC3′; ryk, 5′-GGAGCTGC-AGTCGGCTTCCG-3′ and 5′-GGACTTCGCATGCCAG-GTGAAG-3′; actin, 5′-TTCAACACCCCAGCCATGTA-3′, and 5′-TTGCCAATGGTGATGACCTG-3′. All RT-PCRs were repeated at least three times.

RESULTS

Wnt-5a Induces Thr-34 Phosphorylation of DARPP-32—To test whether recombinant Wnt-5a (rWnt-5) can trigger DARPP-32 phosphorylation, we expressed Myc-tagged DARPP-32 in MCF-7 cells that lack endogenous expression of DARPP-32. These cells have previously been found to be a good model system for functional studies of how DARPP-32 affects cell migration (1). The relative expression levels of endogenous DARPP-32 in different breast epithelial cell lines (Fig. 1*A*, *left*), and the endogenous levels in HB2 and MCF-7 compared with overexpressed DARPP-32 in MCF-7 cells (Fig. 1*A*, *right*) are shown. MCF-7 cells express Wnt-5a (Fig. 1*B*) and exhibit a basal level of Thr-34-DARPP-32 phosphorylation, when DARPP-32 expression is introduced (Fig. 1*C*). Nevertheless, there was a significant increase in Thr-34-DARPP-32 phosphorylation after 5 min of stimulation with different concentrations of rWnt-5a (Fig. 1*C*), demonstrating that the Wnt-5a signaling mechanism can still be activated despite the endogenous expression of this protein. rWnt-5a-stimulated (0.4 μg/ml) Thr-34-DARPP-32 phosphorylation peaked at a ~3-fold increase after 5 min and returned to basal levels after 30 min (Fig. 1*D*). In the same fashion, rWnt-5a was capable of inducing Thr-34 phosphorylation of endogenously expressed DARPP-32 in the non-cancer cell line HB2 (Fig. 1*E*). The Thr-34-phosphorylation of endogenous DARPP-32 in HB2 cells peaked earlier than the Thr-34 phosphorylation of exogenous DARPP-32 in MCF-7 cells. Stimulation with forskolin (1 μM) was used as a positive control (Fig. 1*E*). The second major phosphorylation site of DARPP-32, Thr-75, was unaltered by rWnt-5a stimulation in DARPP-32-expressing MCF-7 cells (Fig. 1*F*). The capacity of rWnt-5a to stimulate DARPP-32 phosphorylation appears to be selective, since recombinant Wnt-3a (rWnt-3a) had no effect on DARPP-32 phosphorylation (Fig. 1*G*).

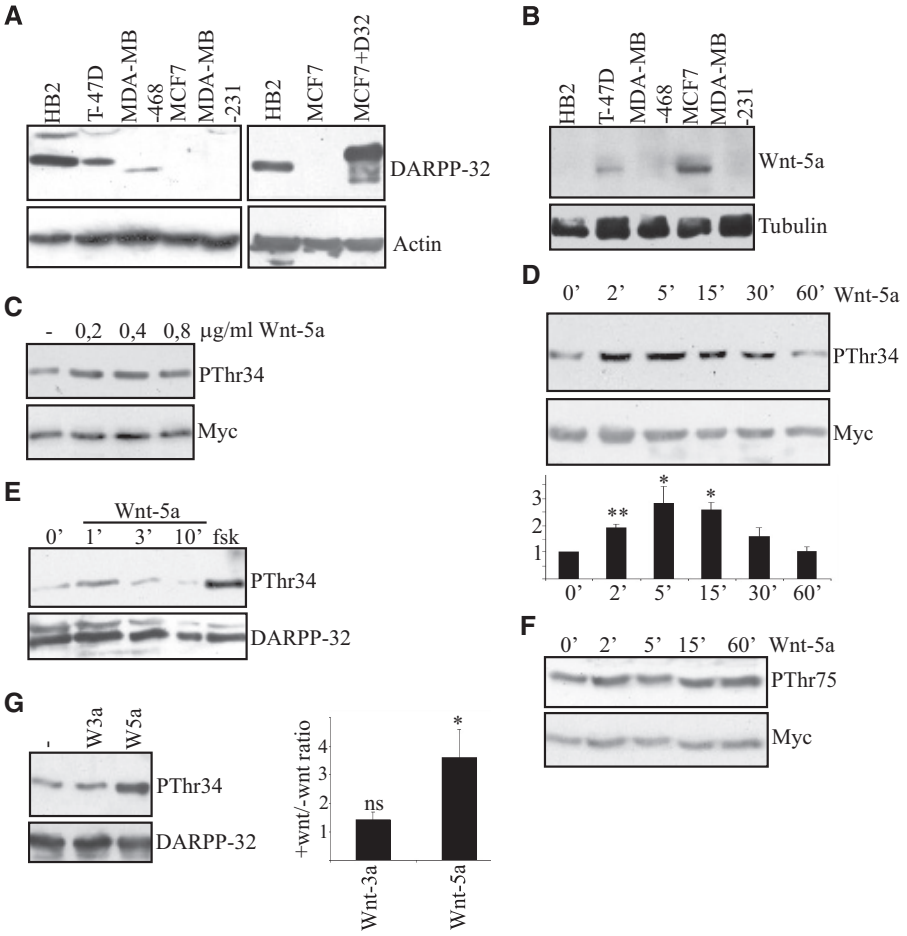

FIGURE 1. **Wnt-5a induces Thr-34 phosphorylation of DARPP-32 in MCF-7 and HB2 breast epithelial cells.** *A, left panel*, expression of DARPP-32 in five different breast epithelial cell lines, detected by anti-DARPP-32 Western blotting. *Right panel*, comparison of endogenous levels of DARPP-32 in HB2 cells to exogenous levels of Myc-tagged DARPP-32 in transfected MCF-7 cells, detected by anti-DARPP-32 Western blotting. *B*, expression of Wnt-5a in five different breast epithelial cell lines, detected by an anti-Wnt-5a antibody. *C*, Western blot showing Thr-34 phosphorylation of DARPP-32 in MCF-7 cells expressing Myc-DARPP-32, after 5 min of stimulation with different concentrations of rWnt-5a, as detected by an anti-phospho-Thr-34-DARPP-32 antibody. *D, upper panel*, Western blot showing the kinetics of Thr-34-DARPP-32 phosphorylation upon stimulation with 0.4 μg/ml rWnt-5a in DARPP-32-expressing MCF-7 cells. *Lower panel*, densitometric analysis of three different Western blots. The data are given as means ± S.D. *E*, Western blot showing Thr-34 phosphorylation of endogenous DARPP-32 induced by Wnt-5a in HB2 cells as detected by anti-phospho Thr-34-DARPP-32 antibody. *F*, Western blot showing the time kinetics of Thr-75 DARPP-32 phosphorylation upon stimulation with 0.4 μg/ml rWnt-5a in Myc-DARPP-32-expressing MCF-7 cells, anti-phospho Thr-75 DARPP-32 antibody. *G, left panel*, Thr-34-DARPP-32 phosphorylation after 5 min of stimulation with either 0.4 μg/ml rWnt-5a or 0.1 μg/ml rWnt-3a. *Right panel*, densitometric analysis of five different Western blots. Wnt-3a or Wnt-5a stimulation was measured relative to no stimulation, which was set to 1. All of the Western blots shown are representative of at least three independent experiments.

Wnt-5a Stimulates Thr34-DARPP-32 Phosphorylation by a cAMP/PKA-dependent Mechanism—Studies of neuronal cells have revealed that Thr-34-DARPP-32 is a PKA target site (2), and we have previously observed that phosphorylation of Thr-34, induced by mammary epithelial cell detachment, requires PKA activity (1). We therefore tested whether inhibition of PKA activity could abrogate rWnt-5a-induced Thr-34 phosphorylation of DARPP-32. Consistent with involvement of PKA, both the inhibitory cAMP analogue RPcAMPS (Fig. 2*A*) and the PKA catalytic site inhibitor H89 (Fig. 2*B*) abolished rWnt-5a induced Thr34-DARPP-32 phosphorylation. These results suggest that Wnt-5a triggers an increase of the intracellular of concentration of cAMP.

To test this hypothesis we applied a novel evanescent wave microscopy method enabling detection of cAMP concentration changes beneath the plasma membrane (20). MCF-7 cells were transfected with a PKA-based fluorescent translocation biosensor that consists of a modified, membrane targeted and CFP-labeled PKA regulatory subunit, and a YFP-labeled catalytic subunit. Stimulation of cAMP formation by activation of adenylyl cyclase with 10 μM forskolin (positive control) resulted in selective loss of membrane YFP fluorescence, reflecting the dissociation of the PKA catalytic subunit from the membrane-anchored regulatory subunit (Fig. 2*C*). Because cAMP does not affect the localization of the regulatory subunit, CFP fluorescence provides a reference and the CFP/YFP fluorescence ratio was used as a measure of the submembrane cAMP concentration after normalization of the prestimulatory ratio to 1. Forskolin (10 μM) induced a sustained 0.38 ± 0.06 (mean ± S.E., $n = 8$) increase in CFP/YFP ratio (Fig. 2*C*), whereas rWnt-5a (0.4 μg/ml) induced a transient elevation of cAMP, which reached a maximal amplitude of 0.24 ± 0.06 ratio units (mean ± S.E., $n = 12$) and typically returned to the baseline within 5 min (Fig. 2*D*). Thus, rWnt-5a induced Thr-34 phosphorylation of DARPP-32 is cAMP/PKA-dependent. To investigate whether this mechanism is executed through a $G\alpha_s$ protein, we down-regulated $G\alpha_s$ with siRNA and analyzed phosphorylation of DARPP-32 induced by Wnt-5a in MCF-7 cells. We observed that reduction of the $G\alpha_s$ protein level strongly suppressed DARPP-32 phosphorylation even in the presence of Wnt-5a stimulation (Fig. 2*E*). These data further support our hypothesis that a Wnt-5a-induced cAMP signaling pathway is responsible for the phosphorylation of DARPP-32.

Wnt-5a Inhibits Cell Migration via DARPP-32—To elucidate whether the rWnt-5a-induced phosphorylation of DARPP-32 plays a role in inhibiting breast cancer cell migration, we used a Boyden chamber assay, allowing the cells to migrate through a collagen-coated membrane for 18 h. Under these conditions, stimulation of control-transfected MCF-7 cells with rWnt-5a significantly reduced cell migration (Fig. 3*A*). As previously reported (1), introduction of DARPP-32 inhibited migration of MCF-7 cells. However, there was no additional effect of rWnt-5a stimulation (Fig. 3*A*, *upper panel*). Since DARPP-32-mediated inhibition of cell migration is strictly dependent on

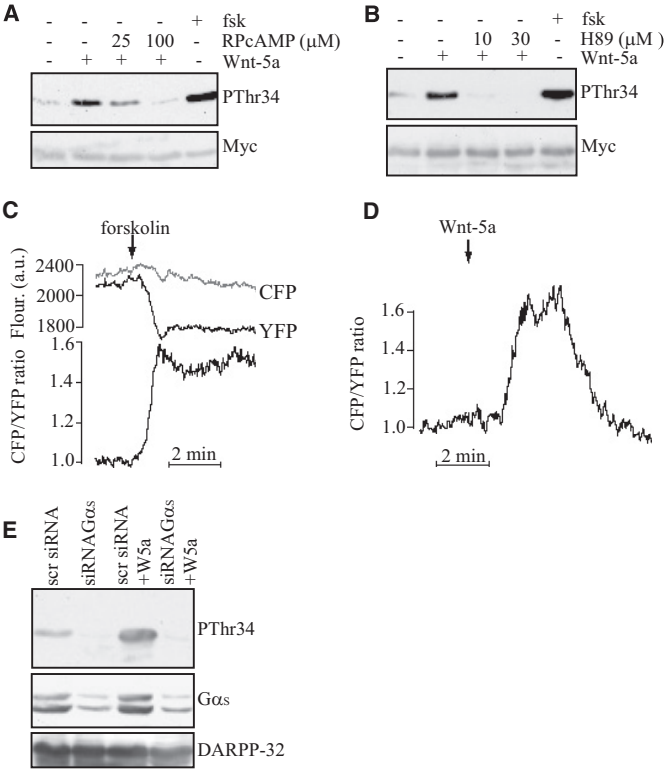

FIGURE 2. **Wnt-5a-induced Thr-34 phosphorylation of DARPP-32 involves cAMP elevation and activation of PKA.** *A*, Western blot showing that the PKA inhibitor RPcAMPS inhibits rWnt-5a-induced Thr-34-DARPP-32 phosphorylation in DARPP-32-expressing MCF-7 cells, as detected by anti-pThr34 antibody. RPcAMPS was added in serum-free medium 1 h prior to stimulation with 0.4 μg/ml rWnt-5a for 5 min. Stimulation with 1 μM forskolin for 20 min was used as a positive control. *B*, Western blot showing H89 inhibition of rWnt-5a-induced pThr34-DARPP-32 phosphorylation in Myc-DARPP-32-expressing MCF-7 cells, as detected by anti-pThr34 antibody. H89 was added in serum-free medium 1 h prior to stimulation with 0.4 μg/ml rWnt-5a for 5 min. Stimulation with 1 μM forskolin for 20 min was used as a positive control. *C* and *D*, evanescent wave microscopy recording of CFP and YFP fluorescence and the cAMP-dependent CFP/YFP ratio from individual MCF-7 cells expressing a fluorescent cAMP biosensor. The cells are stimulated with 10 μM forskolin (*C*, $n = 8$) or 0.4 μg/ml Wnt-5a (*D*, $n = 12$) and the prestimulatory CFP/YFP ratio was normalized to unity. *E*, Thr-34-DARPP-32 phosphorylation after 5 min of stimulation with 0.4 μg/ml rWnt-5a in cells treated with siRNA targeting the $G\alpha_s$ protein or a scrambled sequence as a control. All of the Western blots shown are representative of at least three independent experiments.

phosphorylation of Thr-34-DARPP-32 (1), the lack of an effect of rWnt-5a on DARPP-32-dependent cell migration is probably due to the fact that cell detachment prior to the start of the Boyden-chamber experiment triggered a much higher level of Thr-34 phosphorylation than rWnt-5a stimulation (Fig. 3*A*, *lower panel*).

We therefore decided to test the impact of Wnt-5a/DARPP-32 signaling on cell migration in a wound healing assay, where pThr34-DARPP-32 is at basal levels at the beginning of the experiment. Cells were plated onto collagen-coated dishes overnight to grow to confluency and allow the detachment-induced Thr-34-DARPP-32 phosphorylation to subside (1). We induced a wound by making a scratch through the confluent layer of cells after which wound closure was measured over 24 h. Using this experimental setup we saw an inhibition of cell migration due to rWnt-5a induced phosphorylation of DARPP-32 (Fig. 3*B*). As expected, DARPP-32 did not inhibit migration without rWnt-5a stimulation since the Thr-34 phosphorylation started at basal levels in this assay (Fig. 3*B*). Next, we wanted to test whether down-regulation of DARPP-32 expression in a breast cancer cell line with endogenous expression of DARPP-32 would lead to an increase in cell migration. We used the T47D breast cancer cell line for this purpose and found that depleting these cells of DARPP-32 led to an increase in migration (Fig. 3*C*), thus confirming the results from the MCF-7 cell migration assay studies.

DARPP-32 Interacts with PP1 in a Phospho-Thr-34-dependent Manner—From neuronal studies, it is known that phospho-Thr34-DARPP-32 can bind to and inhibit the activity of PP1 (3). To investigate whether PP1 and DARPP-32 interact in a similar fashion in breast cancer cells, we performed an anti-PP1 immunoprecipitation on MCF-7 cells transfected with either T34A-DARPP-32 or wt-DARPP-32 vectors. Surprisingly, T34A-DARPP-32 could still bind PP1, which might be due to an N-terminal PP1 docking motif on DARPP-32 (Fig. 4). However, binding to T34A-DARPP-32 is not sufficient to inhibit PP1, since the phospho-Thr34 group is required to sterically block the catalytic site of PP1 (24). MCF-7 cells transfected with wt-DARPP-32 were left unstimulated, or stimulated with rWnt-5a (0.4 μg/ml) or forskolin (1 μM). We noted a significant interaction between PP1 and DARPP-32 in unstimulated cells and a slight increase in rWnt-5a stimulated cells. In forskolin-stimulated cells on the other hand, we co-immunoprecipitated significantly more DARPP-32 with PP1 compared with unstimulated cells (Fig. 4). These findings led us to investigate possible PP1 targets that could be involved in the regulation of cell migration. Because CREB activity is suppressed in DARPP-32 knock-out mice (5), we wanted to test whether CREB might be implicated in this process.

Wnt-5a Induces CREB Activity, Which Is Enhanced by DARPP-32—Inhibition of PP1 can lead to increased CREB activity (pSer133-CREB), since PP1 is responsible for dephosphorylation of pSer133-CREB (25). We speculated that such a mechanism could explain how Wnt-5a induced Thr34-DARPP-32 phosphorylation affects cell migration. rWnt-5a stimulation of MCF-7 cells lacking DARPP-32 led to increased phosphorylation of CREB, peaking at 10 min (Fig. 5*A*). Moreover, rWnt-5a stimulation of DARPP-32-expressing MCF-7 cells further enhanced CREB activity, compared with cells where DARPP-32 was expressed without rWnt-5a (Fig. 5*B*). The finding that rWnt-5a can trigger CREB activity in the absence of DARPP-32 is novel and may reflect the Wnt-5a-induced activation of PKA, since this kinase has been shown to phosphorylate CREB at the Ser-133 site (26). Consequently, the present study suggests that PKA has a dual role in the activation of CREB, acting both via direct phosphorylation of Ser-133-CREB and via phosphorylation of Thr-34-DARPP-32 that then inhibits Ser-133-CREB dephosphorylation by suppressing PP1 phosphatase activity.

Dominant Negative CREB Diminishes Wnt-5a/DARPP-32-mediated Inhibition of Cell Migration—To test whether Wnt-5a/DARPP-32 mediated inhibition of cell migration is dependent on CREB activity, we transfected MCF-7 cells with empty vector, DARPP-32 vector, or DARPP-32 and DN-CREB vectors. These cells were then stimulated with rWnt-5a and their ability to migrate was compared in a wound-healing assay. The

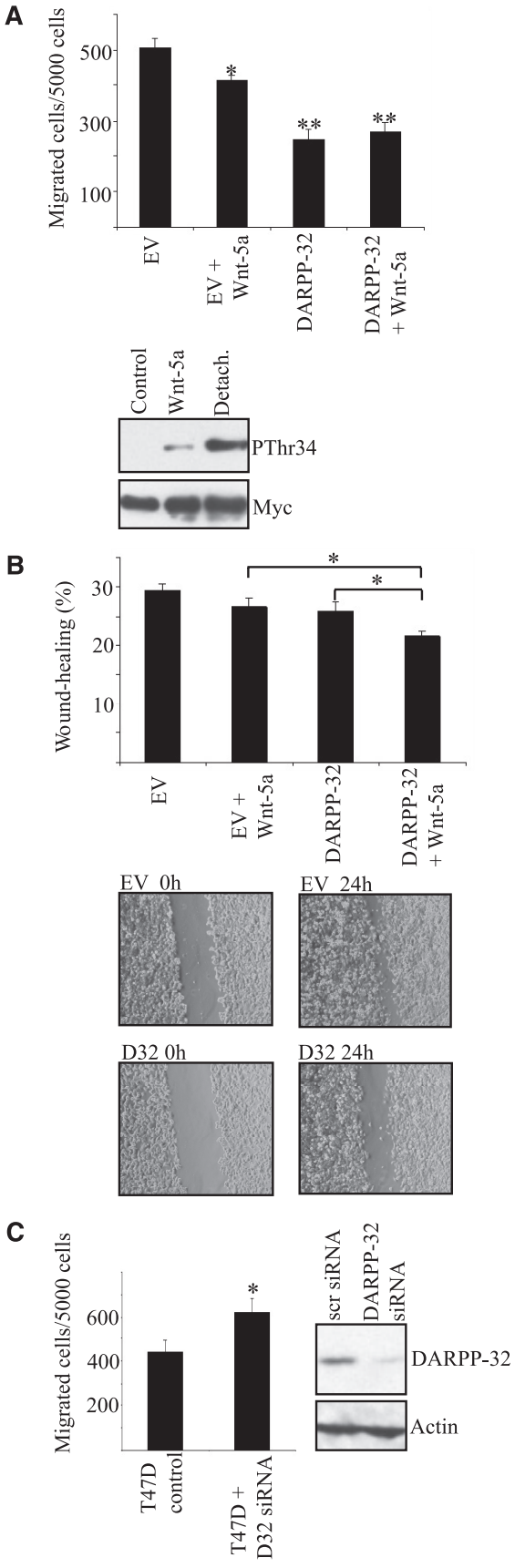

FIGURE 3. **Wnt-5a induced phosphorylation of DARPP-32 leads to inhibition of cell migration.** *A*, *upper panel*, migration of MCF-7 cells transfected with Myc-DARPP-32 or empty vector through collagen-coated wells ($n = 8$). All statistical significances were calculated in comparison with the empty vector control; *Lower panel*, Western blot showing comparison of rWnt-5a and detachment induced pThr34-phosphorylation, as detected by anti-pThr34 antibody. *B*, *upper panel*, wound-healing assay on MCF-7 cells in collagen-coated plates, transfected with either empty vector or Myc-DARPP-32 and left untreated or stimulated with 0.4 μg/ml rWnt-5a for 24 h ($n = 12$); *lower panel*, representative photographs from the wound-healing experiments. *C*, *left panel*, migration of T47D cells expressing endogenous DARPP-32 or depleted for DARPP-32 by siRNA targeting ($n = 6$), *right panel*, DARPP-32 expression level in T47D cells treated with siRNA targeting DARPP-32 or a scrambled control sequence. Both of the Western blots shown are representative of at least three independent experiments.

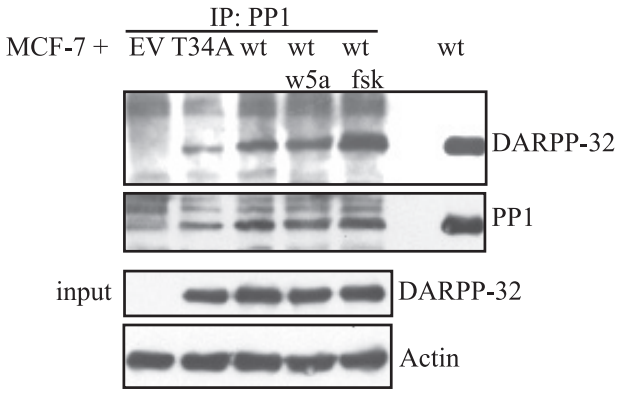

FIGURE 4. **DARPP-32 interacts with PP1 in MCF-7 cells.** *Upper panel*, co-immunoprecipitation of PP1 and DARPP-32. MCF-7 cells transfected with either empty vector, Myc-T34ADARPP-32, or Myc-DARPP-32 expression plasmid. Binding of PP1 to DARPP-32 was verified by anti-PP1 immunoprecipitation followed by anti-DARPP-32 Western blotting. *Lower panel*, aliquots of the lysates to be used for immunoprecipitation experiments were tested for Myc-DARPP-32 expression to verify equal DARPP-32 levels in all Myc-DARPP-32-expressing MCF-7 lysates. The Western blot shown is a representative of three independent co-immunoprecipitation experiments.

results revealed that DARPP-32-expressing cells, but not DARPP-32/DN-CREB-expressing cells, migrated significantly less than empty vector-transfected cells (Fig. 5*C*). We conclude that CREB activity plays an important role in Wnt-5a/DARPP-32-mediated inhibition of cell migration. To further consolidate these findings we also explored whether detachment-induced Thr-34-DARPP-32 phosphorylation and inhibition of cell migration was dependent on CREB activity. We performed a Boyden chamber assay with MCF-7 cells transfected with empty vector, DARPP-32 vector or DARPP-32 and DN-CREB vectors. The results were similar to those obtained in the wound-healing assay in the sense that DARPP-32-expressing but not DARPP-32/DN-CREB-expressing cells migrated significantly less than empty vector transfected MCF-7 cells (Fig. 5*D*). Thus, CREB activity is important for DARPP-32-mediated inhibition of cancer cell migration.

Phospho-Thr-34-DARPP-32 Suppresses Filopodia Formation—To explore the effect of phospho-Thr-34-DARPP-32 on single cell morphology, we immunostained DARPP-32 transfected MCF-7 cells that had been detached and allowed to adhere to collagen-coated glass slides overnight. The cells were incubated in the absence or presence of 1 μM forskolin for 20 min to re-trigger Thr34-DARPP-32 phosphorylation, and subsequently fixed and stained with antibodies and phalloidin. Because the slides had both DARPP-32-transfected and non-transfected cells, the two cell types could be directly compared. We first ensured that phosphorylated DARPP-32 was only

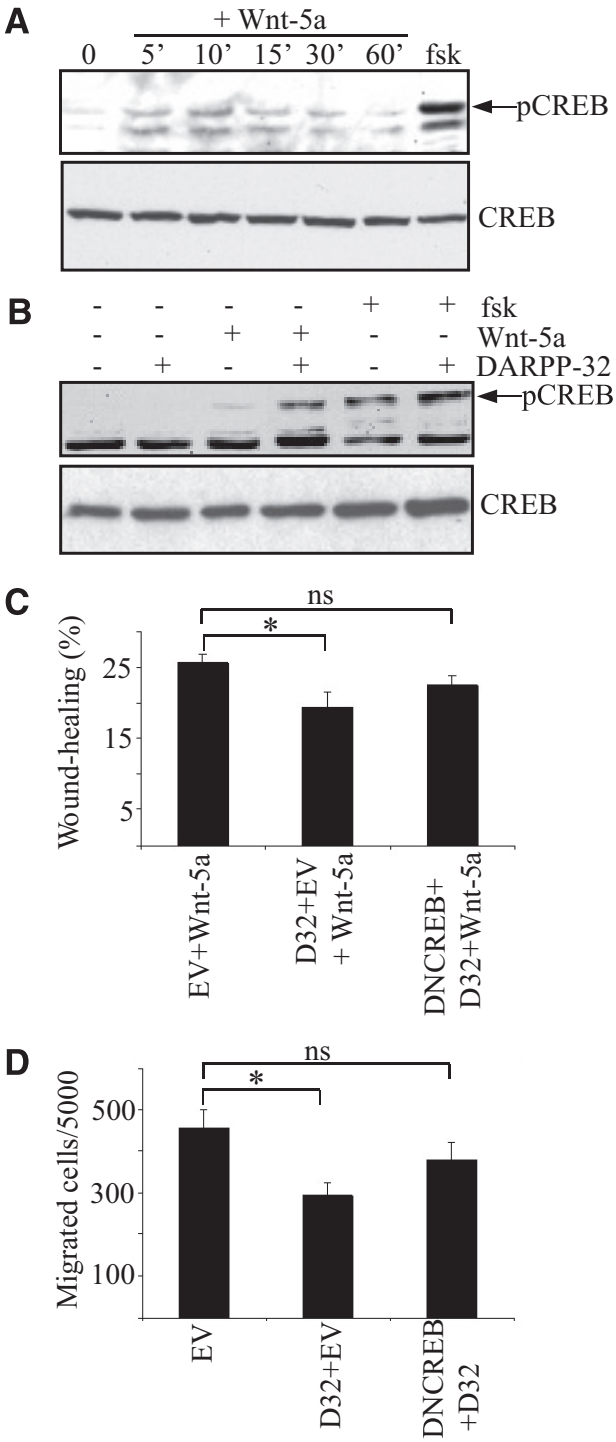

FIGURE 5. **Involvement of CREB in Wnt-5a- and DARPP-32-mediated inhibition of cell migration.** *A*, Western blot showing rWnt-5a-induced CREB phosphorylation in MCF-7 cells, as detected by anti-pCREB antibody. *B*, Western blot showing CREB phosphorylation in MCF-7 cells transfected with empty vector or Myc-DARPP-32 expression plasmid, non-stimulated or stimulated with 0.4 μg/ml rWnt-5a for or 1 μM forskolin for 10 min. Each Western blot is representative of six independent experiments. *C*, wound-healing assay with MCF-7 cells in collagen-coated plates, transfected with either empty vector, Myc-DARPP-32 vector, or both Myc-DARPP-32 and DN-CREB vectors. All cells were stimulated with 0.4 μg/ml rWnt-5a for 24 h (n = 12). *D*, migration of MCF-7 through collagen-coated wells transfected with empty vector, Myc-DARPP-32 vector, or both Myc-DARPP-32 and DN-CREB vectors (n = 6).

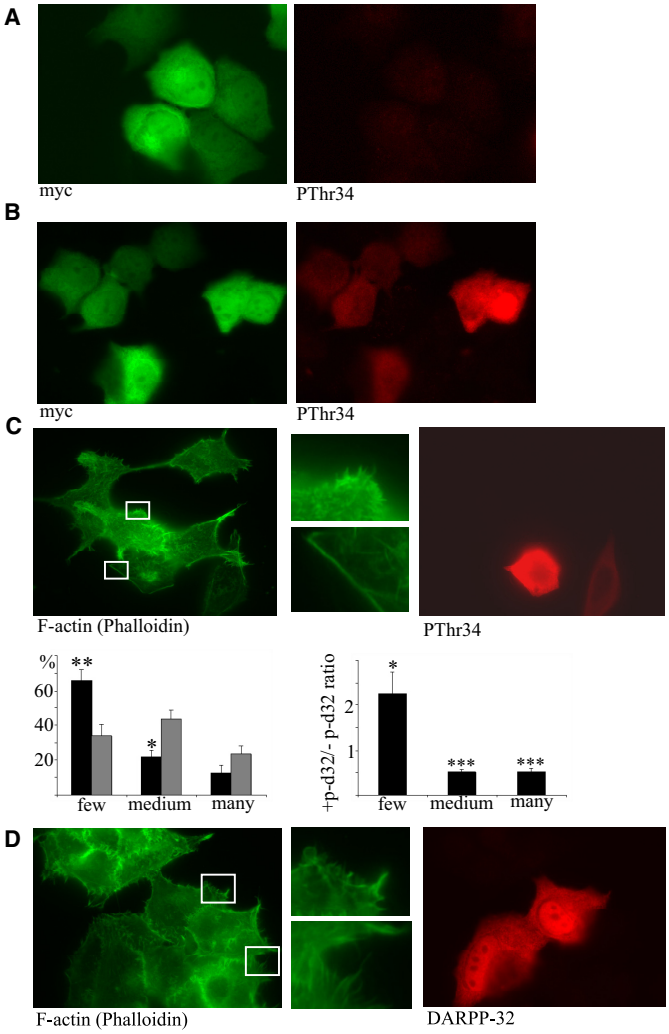

FIGURE 6. **Thr-34 phosphorylation of DARPP-32 leads to inhibition of filopodia formation.** MCF-7 cells expressing Myc-DARPP-32 were plated onto collagen-coated glass slides overnight. *A*, non-stimulated cells or *B*, cells stimulated with 1 μM forskolin for 20 min were fixed and stained for Myc and pThr34-DARPP-32. *C*, *upper panel*, cells expressing Myc-DARPP-32 were stimulated with 1 μM forskolin for 20 min were fixed and stained for F-actin (with FITC-phalloidin) and pThr34-DARPP-32. *Lower panel*, quantitative analysis of filopodia formation in pThr34-DARPP-32-positive and -negative MCF-7 cells. The *left panel* gives the percentage of cells in each category (*black bars*: + pThr34-DARPP-32, *gray bars*: - pThr34-DARPP-32). The *right panel* gives the ratio of pThr34-DARPP-32-positive to pThr34-DARPP-32-negative for each category. *D*, Myc-T34A-DARPP-32 was expressed in MCF-7 cells, and cells were plated onto collagen-coated glass slides overnight, stimulated with 1 μM forskolin for 20 min, fixed, and stained F-actin (with FITC-phalloidin) and DARPP-32 (n = 5 for all experiments in this figure).

detected in transfected cells stimulated with forskolin (Fig. 6*A*, nonstimulated and *B*, stimulated). Staining of DARPP-32-expressing MCF-7 cells with phalloidin (for F-actin) and anti-pThr-34-DARPP-32 revealed that phospho-DARPP-32-expressing MCF-7 cells show less filopodia formation than non-transfected cells (Fig. 6*C*). Immunostaining of T34A-DARPP-32-expressing MCF-7 cells with an anti-DARPP-32 antibody, revealed that these cells had no alteration in filopodia formation in relation to non-transfected cells (Fig. 6*D*), thus confirming the phospho-Thr-34-DARPP-32 specificity of this phenotype. Wnt-5a stimulation for 24 h also caused a reduction in filopodia of DARPP-32-expressing cells compared with non-expressing MCF-7 cells (Fig. 7*A*). To check whether this

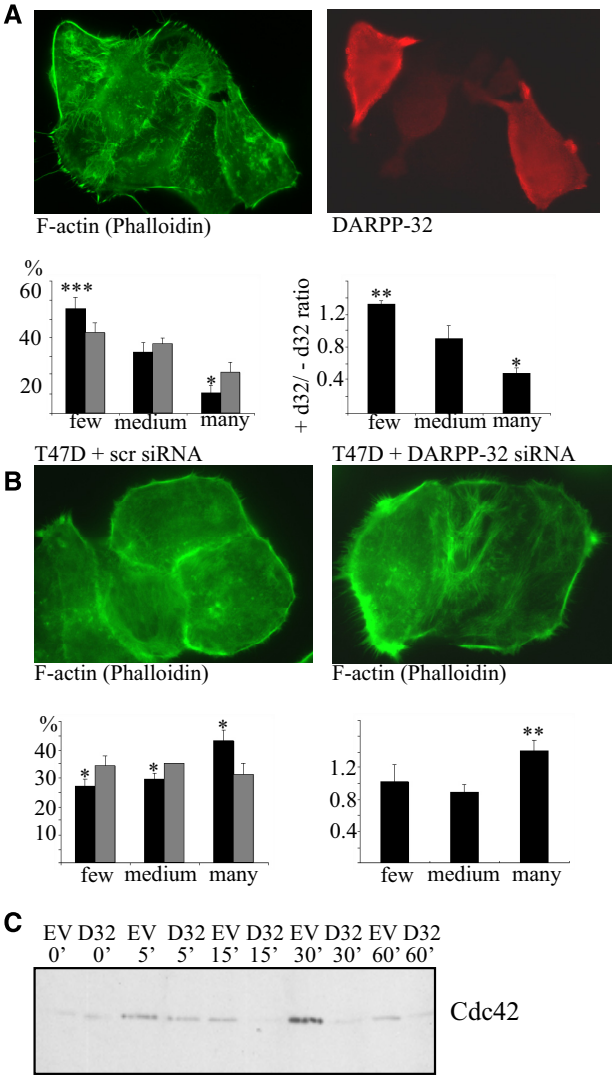

FIGURE 7. **Effect of Wnt-5a and involvement of DARPP-32 and CDC42 in filopodia formation.** *A*, *upper panel*, Myc-DARPP-32 was expressed in MCF-7 cells, that were then plated onto collagen-coated glass slides overnight and subsequently stimulated with 0.4 μg/ml Wnt-5a for 24 h before being fixed and stained for F-actin (with FITC-phalloidin) and DARPP-32. *Lower panel*, quantitative analysis of filopodia formation in DARPP-32-positive and -negative MCF-7 cells. The *left panel* gives the percentage of cells in each category (*black bars*: + DARPP-32, *gray bars*: - DARPP-32) ($n = 5$). The *right panel* gives the ratio of DARPP-32-positive to DARPP-32-negative for each category. *B*, *upper panel*, T47D cells were treated with siRNA against DARPP-32 or scrambled control siRNA and stained for F-actin by FITC-phalloidin. *Lower panel*, quantitative analysis of filopodia formation in DARPP-32 siRNA- or scrambled siRNA-treated T47D cells. The *left panel* gives the percentage of cells in each category (*black bars*: DARPP-32 siRNA, *gray bars*: scrambled siRNA) ($n = 5$). The *right panel* gives the ratio of DARPP-32 siRNA to scrambled siRNA for each category. *C*, MCF-7 cells transfected with either Myc-DARPP-32 expression vector or empty vector were detached and re-plated onto collagen-coated plates for 0–60 min. Cells were lysed, and active Cdc42 was precipitated in a GST-PAK1 pull-down assay. A representative anti-Cdc42 Western blot of these pulldowns ($n = 5$) is shown.

effect could be reversed by down-regulation of endogenous DARPP-32 in cancer cells, we analyzed filopodia formation of T47D control cells or T47D cells depleted for DARPP-32 by siRNA targeting (Fig. 3*C*). The result showed that T47D DARPP-32-negative cells have more filopodia than T47D control cells, when evaluated quantitatively as described above (Fig. 7*B*), confirming that DARPP-32 negatively regulates filopodia formation. It has previously been documented that the Rho GTPase Cdc42 plays a central role in filopodia formation (27). In agreement, we saw that DARPP-32-expressing MCF-7 cells had a lower Cdc42 activity level than empty vector-transfected control cells (Fig. 7*C*).

There are several potential receptors and co-receptors that could mediate Wnt-5a-induced effects in breast cancer cells. To address which of these receptors mediates Wnt-5a-induced cAMP production and phosphorylation of DARPP-32, we first evaluated their expression in MCF-7 and T47D cells by Western blotting and RT-PCR. Ror2 was not expressed in MCF-7 cells, whereas ryk was expressed in both cell lines (Fig. 8*A*). Expression of the Frizzled receptors 2–5 that has previously been linked to Wnt-5a signaling, were tested by RT-PCR. Both cell lines clearly expressed Frizzled-3 and -4, whereas only a faint band was seen for Frizzled-2 in both cell lines. The Frizzled-5 receptor was only detected in MCF-7 cells (Fig. 8*B*). Very little is currently known about Frizzled-receptors with regard to cAMP signaling. However, a structure-function analysis of 10 Frizzled receptors by Malbon and co-workers (28) has revealed that the Frizzled-3 receptor is the most likely candidate to associate with and activate $G\alpha_s$ and cAMP signaling. We therefore decided to knock down Frizzled-3 by siRNA targeting (Fig. 8*C*). Indeed, Frizzled-3 down-regulation completely abolished Wnt-5a-induced phosphorylation of DARPP-32, and we conclude that Frizzled-3 is responsible for the Wnt-5a-induced cAMP signal that leads to DARPP-32 phosphorylation (Fig. 8*D*).

DISCUSSION

Here we show that Wnt-5a induces a cAMP response leading to Thr-34 phosphorylation of DARPP-32 and a subsequent downstream activation of CREB resulting in inhibition of breast cancer cell migration. Wnt-5a was found to generate cAMP beneath the plasma membrane in MCF-7 cells, and two different unrelated inhibitors of cAMP/PKA signaling suppressed the Wnt-5a-induced Thr-34-DARPP-32 phosphorylation in this breast cancer cell line. Furthermore, we demonstrated that Wnt-5a-induced phosphorylation of DARPP-32 can be abolished by siRNA-mediated knockdown of either $G\alpha_S$ or Frizzled-3, demonstrating a novel Wnt-5a-induced Frizzled-3-dependent cAMP signaling pathway.

A recent study reported that PKA and CREB can act downstream of Wnt-5a in human dermal fibroblasts. However, the authors did not outline the signaling mechanism responsible for their observations (29). In general, very few studies have investigated Wnt activation of cAMP signaling, presumably due to a lack of sufficiently sensitive assays to detect changes in cAMP. Despite this, an interesting study of Wnt/cAMP signaling showed that phospho-Ser-133-CREB staining patterns of mouse embryos coincided with areas of myogenic induction and Wnt protein staining (30). Furthermore, the authors found that Wnt-1 and Wnt-7a are important for myogenesis of mouse embryos in a strictly PKA and CREB-dependent manner (30).

A major function of the cAMP/PKA-triggered Thr34-DARPP-32 phosphorylation is the inhibition of PP1 phosphatase activity (5). Since PP1 is ubiquitously expressed, and DARPP-32 expression has been found in many tissues including brain, breast, esophagus, pancreas, thyroid, kid-

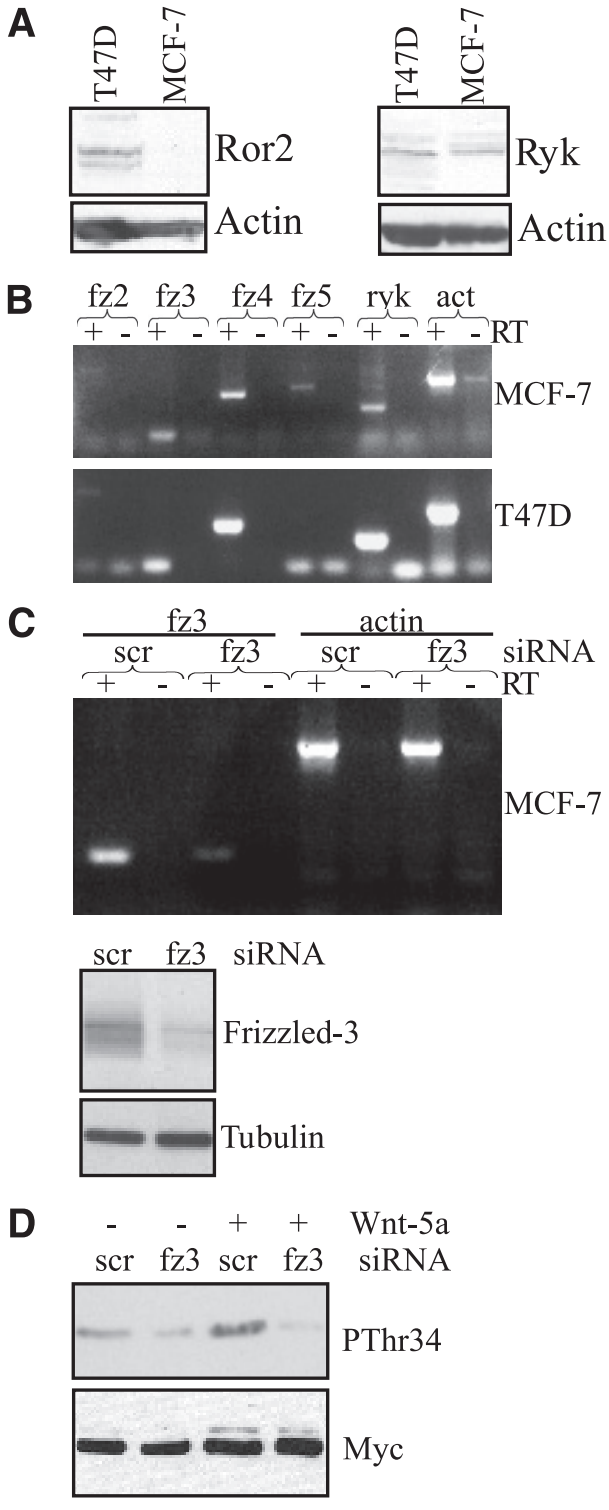

FIGURE 8. **Frizzled-3 mediates Wnt-5a-induced phosphorylation of DARPP-32.** *A*, Western blots showing Ror2 and Ryk expression in MCF-7 and T47D cells. *B*, RT-PCR expression analysis of Frizzled -2,-3,-4,-5, Ryk, and actin. For each expression analysis a negative control lacking reverse transcriptase (−*RT*) has been included. *C*, *upper panel*, RT-PCR of Frizzled-3 in MCF-7 cells transfected with either Frizzled-3 or scrambled siRNA. Actin served as a positive control and for each expression analysis a negative control lacking reverse transcriptase (−*RT*) has been included. *Lower panel*, knockdown of Frizzled-3 expression in MCF-7 cells verified by Western blot analysis using an anti-Frizzled-3 antibody. *D*, Western blot analysis showing Wnt-5a (0.4 μg/ml, 5 min)-mediated Thr-34 phosphorylation in DARPP-32-expressing MCF-7 cells co-transfected with either Frizzled-3 siRNA or scrambled siRNA. The Western blots and RT-PCRs shown are representative of at least three independent experiments.

ney, fat, ovary, and colon (1, 6, 9, 10, 31–36), DARPP-32 could have an important role in restricting cell migration in many tissues. The identification of DARPP-32 as an antimigratory protein is novel, but other PP1 inhibitors closely related to DARPP-32 have also been shown to regulate cell migration via inhibition of PP1. Inhibitor-I was recently found to regulate neurite growth cone motility and guidance (37), and Inhibitor-2 has been found to regulate sperm motility (38). In the context of Wnt signaling it is interesting that PP1 was recently found in a screen for proteins inducing β-catenin stabilization. It does so by dephosphorylating Axin, making Axin less accessible for GSK-3β to bind, resulting in decreased β-catenin phosphorylation and consequently β-catenin accumulation. Particularly interesting, the authors could show that co-expression of Inhibitor-2 increased GSK-3β association with PP1 (39). Taken together with our results, these findings suggest that non-canonical Wnt signaling might antagonize canonical Wnt signaling via activation of PP1 inhibitors like DARPP-32 and inhibitor-2.

Remodelling of the actin-cytoskeleton is one of the most central mechanisms in cell migration and in search for such changes induced by DARPP-32 phosphorylation, we stained for F-actin and found that filopodia formation was severely diminished in these cells. In agreement, we show that DARPP-32 inhibits Cdc42 activity, the major GTPase responsible for filopodia formation (27). As the response that led to inhibition of Cdc42 activity was within 1 h, we believe that the initial antimigratory effect of DARPP-32 relates to its ability to inhibit Cdc42 activity and filopodia formation. Furthermore, our results suggest that CREB is another important target molecule in Wnt-5a/DARPP-32-mediated inhibition of breast cancer cell migration, since DN-CREB completely blocked this response. We believe that two signaling mechanisms synergistically act to induce CREB phosphorylation. In addition to stimulating direct phosphorylation of CREB, the increased PKA activity induced by Wnt-5a inhibits PP1 via phosphorylation of DARPP-32. Wnt-5a-mediated cAMP generation therefore provides a straightforward explanation for activation of CREB via PKA and demonstrates a mechanism whereby PKA can both directly cause activation of a downstream protein and enhance its own effect by inhibiting the antagonizing enzyme, PP1. Most functional studies of CREB have been focused on learning, memory, and cell survival (40, 41). In contrast, very few studies have been performed on the role of CREB in cell migration, and the results are inconsistent. Thus, CREB has been reported to both promote (42) and inhibit (43) smooth muscle cell migration. However, nothing is known about the CREB induced transcriptional targets that are expressed and responsible for modifying cell migration. Clearly, the identification of these targets is an important goal for our understanding of why CREB can affect cell migration differently depending on cell type and the circumstances under which it is activated. In summary, we believe that there are at least two different signaling pathways leading to Wnt-5a/DARPP-32 mediated inhibition of breast cancer cell migration: a faster transcriptionally independent Cdc42 pathway and a transcriptionally dependent CREB pathway as illustrated in Fig. 9.

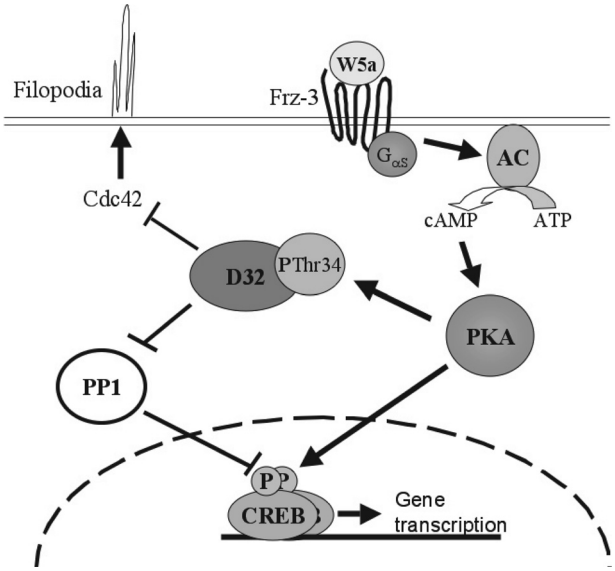

FIGURE 9. **Model of Wnt-5a/DARPP-32-mediated inhibition of breast cancer cell migration.** Autocrine or paracrine acting Wnt-5a ligand activates Frizzled-3 receptors that via $G\alpha_s$ stimulates cAMP formation by adenylyl cyclases (*AC*). cAMP activates PKA, which phosphorylates DARPP-32 at Thr-34 and CREB at Ser-133. pThr34-DARPP-32 suppresses filopodia formation in part by reducing CDC42 activity. In addition, pThr34-DARPP-32 inhibits PP1, which in turn leads to enhanced CREB phosphorylation. CREB mediates transcription of genes that also regulate cell migration by an as yet unidentified mechanism.

Our previous and present results reveal an intimate interaction between Wnt-5a, DDR1, and DARPP-32 in cell signaling. DARPP-32 binds to DDR1 with weaker affinity when DDR1 is activated by collagen (1), and since Wnt-5a expression increases collagen-induced DDR1 phosphorylation, this could mean that Wnt-5a induces release of DARPP-32 from DDR1 to target sites in the cell. A strong argument for an important role of DDR1 in this signaling circuit comes from our study in MDA-MB-231 cells that lack endogenous expressions of both DARPP-32 and DDR1. Introduction of DARPP-32 in these cells does not inhibit cell migration unless DDR1 is co-expressed. We believe that the role of Wnt-5a activation of phosphorylation of DARPP-32 could be to mediate a signal that makes breast epithelial cells stay attached to the basement membrane. The interplay of Wnt-5a and DARPP-32 with DDR1, which is activated by collagen IV in the basement membrane, could be crucial for the adhesive properties of the cell. In this model, it stands to reason that cell detachment mediates a far stronger phosphorylation of DARPP-32 than Wnt-5a, to force the detached breast epithelial cell to re-attach to the basement membrane. Such mechanisms would act to prevent breast cancer metastasis, since transformed breast epithelial cells need to detach from the basement membrane as an initial step in the metastatic process. In conclusion we have established that Wnt-5a stimulation induces a Frizzled-3- and $G\alpha_s$-dependent cAMP signal that, via PKA, leads to phosphorylation and activation of both DARPP-32 and CREB. DARPP-32 activity functions to inhibit Cdc42 activity and to further potentiate the Wnt-5a-induced activation of CREB. These signaling events act together to prevent breast cancer cell migration. Pharmacological activation of these pathways could constitute a novel way of limiting breast cancer metastasis.

Acknowledgments—We thank Dr. J. Taylor-Papadimitriou (Imperial Cancer Research Fund, United Kingdom) for providing the HB2 cell line and Dr. Jeffrey S. Rubin (National Institutes of Health) for the kind gift of the anti-Frizzled 3 antibody.

REFERENCES

1. Hansen, C., Greengard, P., Nairn, A. C., Andersson, T., and Vogel, W. F. (2006) *Exp. Cell Res.* **312,** 4011–4018
2. Walaas, S. I., Aswad, D. W., and Greengard, P. (1983) *Nature* **301,** 69–71
3. Hemmings, H. C., Jr., Greengard, P., Tung, H. Y., and Cohen, P. (1984) *Nature* **310,** 503–505
4. Bibb, J. A., Snyder, G. L., Nishi, A., Yan, Z., Meijer, L., Fienberg, A. A., Tsai, L. H., Kwon, Y. T., Girault, J. A., Czernik, A. J., Huganir, R. L., Hemmings, H. C., Jr., Nairn, A. C., and Greengard, P. (1999) *Nature* **402,** 669–671
5. Svenningsson, P., Nishi, A., Fisone, G., Girault, J. A., Nairn, A. C., and Greengard, P. (2004) *Annu. Rev. Pharmacol. Toxicol.* **44,** 269–296
6. Beckler, A., Moskaluk, C. A., Zaika, A., Hampton, G. M., Powell, S. M., Frierson, H. F., Jr., and El-Rifai, W. (2003) *Cancer* **98,** 1547–1551
7. El-Rifai, W., Smith, M. F., Jr., Li, G., Beckler, A., Carl, V. S., Montgomery, E., Knuutila, S., Moskaluk, C. A., Frierson, H. F., Jr., and Powell, S. M. (2002) *Cancer Res.* **62,** 4061–4064
8. Li, L., Miyamoto, M., Ebihara, Y., Mega, S., Takahashi, R., Hase, R., Kaneko, H., Kadoya, M., Itoh, T., Shichinohe, T., Hirano, S., and Kondo, S. (2006) *World J. Surg.* **30,** 1672–1679; discussion 1680–1681
9. Ebihara, Y., Miyamoto, M., Fukunaga, A., Kato, K., Shichinohe, T., Kawarada, Y., Kurokawa, T., Cho, Y., Murakami, S., Uehara, H., Kaneko, H., Hashimoto, H., Murakami, Y., Itoh, T., Okushiba, S., Kondo, S., and Katoh, H. (2004) *Br. J. Cancer* **91,** 119–123
10. Garcia-Jiménez, C., Zaballos, M. A., and Santisteban, P. (2005) *Mol. Endocrinol.* **19,** 3060–3072
11. Li, C., Xiao, J., Hormi, K., Borok, Z., and Minoo, P. (2002) *Dev. Biol.* **248,** 68–81
12. Roarty, K., and Serra, R. (2007) *Development* **134,** 3929–3939
13. Liang, H., Chen, Q., Coles, A. H., Anderson, S. J., Pihan, G., Bradley, A., Gerstein, R., Jurecic, R., and Jones, S. N. (2003) *Cancer Cell* **4,** 349–360
14. Kurayoshi, M., Oue, N., Yamamoto, H., Kishida, M., Inoue, A., Asahara, T., Yasui, W., and Kikuchi, A. (2006) *Cancer Res.* **66,** 10439–10448
15. Kremenevskaja, N., von, Wasielewski, R., Rao, A. S., Schöfl, C., Andersson, T., and Brabant, G. (2005) *Oncogene* **24,** 2144–2154
16. Säfholm, A., Leandersson, K., Dejmek, J., Nielsen, C. K., Villoutreix, B. O., and Andersson, T. (2006) *J. Biol. Chem.* **281,** 2740–2749
17. Jönsson, M., Dejmek, J., Bendahl, P. O., and Andersson, T. (2002) *Cancer Res.* **62,** 409–416
18. Jönsson, M., and Andersson, T. (2001) *J. Cell Sci.* **114,** 2043–2053
19. Hou, G., Vogel, W., and Bendeck, M. P. (2001) *J. Clin. Invest.* **107,** 727–735
20. Dyachok, O., Isakov, Y., Sågetorp, J., and Tengholm, A. (2006) *Nature* **439,** 349–352
21. Snyder, G. L., Girault, J. A., Chen, J. Y., Czernik, A. J., Kebabian, J. W., Nathanson, J. A., and Greengard, P. (1992) *J. Neurosci.* **12,** 3071–3083
22. Valjent, E., Pascoli, V., Svenningsson, P., Paul, S., Enslen, H., Corvol, J. C., Stipanovich, A., Caboche, J., Lombroso, P. J., Nairn, A. C., Greengard, P., Hervé, D., and Girault, J. A. (2005) *Proc. Natl. Acad. Sci. U.S.A.* **102,** 491–496
23. Endo, Y., Beauchamp, E., Woods, D., Taylor, W. G., Toretsky, J. A., Uren, A., and Rubin, J. S. (2008) *Mol. Cell. Biol.* **28,** 2368–2379
24. Huang, H. B., Horiuchi, A., Watanabe, T., Shih, S. R., Tsay, H. J., Li, H. C., Greengard, P., and Nairn, A. C. (1999) *J. Biol. Chem.* **274,** 7870–7878
25. Hagiwara, M., Alberts, A., Brindle, P., Meinkoth, J., Feramisco, J., Deng, T., Karin, M., Shenolikar, S., and Montminy, M. (1992) *Cell* **70,** 105–113
26. Yamamoto, K. K., Gonzalez, G. A., Biggs, W. H., 3rd, and Montminy, M. R. (1988) *Nature* **334,** 494–498
27. Nobes, C. D., and Hall, A. (1995) *Cell* **81,** 53–62
28. Wang, H. Y., Liu, T., and Malbon, C. C. (2006) *Cell Signal* **18,** 934–941
29. Torii, K., Nishizawa, K., Kawasaki, A., Yamashita, Y., Katada, M., Ito, M., Nishimoto, I., Terashita, K., Aiso, S., and Matsuoka, M. (2008) *Cell Signal.* **20,** 1256–1266

30. Chen, A. E., Ginty, D. D., and Fan, C. M. (2005) *Nature* **433,** 317–322
31. Walaas, S. I., Nairn, A. C., and Greengard, P. (1983) *J. Neurosci.* **3,** 291–301
32. Lilja, L., Meister, B., Berggren, P. O., and Bark, C. (2005) *Biochem. Biophys. Res. Commun.* **329,** 673–677
33. Meister, B., Askergren, J., Tunevall, G., Hemmings, H. C., Jr., and Greengard, P. (1991) *J. Endocrinol. Invest.* **14,** 655–661
34. Aperia, A., Hökfelt, T., Meister, B., Bertorello, A., Fryckstedt, J., Holtbäck, U., and Seri, I. (1990) *Am. J. Hypertens.* **3,** 11S–13S
35. Brady, M. J., Nairn, A. C., and Saltiel, A. R. (1997) *J. Biol. Chem.* **272,** 29698–29703
36. Mayerhofer, A., Fritz, S., Mani, S., Rajendra Kumar, T., Thalhammer, A., Ingrassia, P., Fienberg, A. A., and Greengard, P. (2004) *Exp. Clin. Endocrinol. Diabetes* **112,** 451–457
37. Han, J., Han, L., Tiwari, P., Wen, Z., and Zheng, J. Q. (2007) *J. Cell Biol.* **176,** 101–111
38. Vijayaraghavan, S., Stephens, D. T., Trautman, K., Smith, G. D., Khatra, B., da Cruz e Silva, E. F., and Greengard, P. (1996) *Biol. Reprod.* **54,** 709–718
39. Luo, W., Peterson, A., Garcia, B. A., Coombs, G., Kofahl, B., Heinrich, R., Shabanowitz, J., Hunt, D. F., Yost, H. J., and Virshup, D. M. (2007) *EMBO J.* **26,** 1511–1521
40. Dash, P. K., Hochner, B., and Kandel, E. R. (1990) *Nature* **345,** 718–721
41. Jean, D., Harbison, M., McConkey, D. J., Ronai, Z., and Bar-Eli, M. (1998) *J. Biol. Chem.* **273,** 24884–24890
42. Jalvy, S., Renault, M. A., Leen, L. L., Belloc, I., Bonnet, J., Gadeau, A. P., and Desgranges, C. (2007) *Cardiovasc. Res.* **75,** 738–747
43. Klemm, D. J., Watson, P. A., Frid, M. G., Dempsey, E. C., Schaack, J., Colton, L. A., Nesterova, A., Stenmark, K. R., and Reusch, J. E. (2001) *J. Biol. Chem.* **276,** 46132–46141